

Matrix Metalloproteinase Gelatinase B (MMP-9) Coordinates and Effects Epithelial Regeneration*

Received for publication, August 9, 2001, and in revised form, October 28, 2001
Published, JBC Papers in Press, October 31, 2001, DOI 10.1074/jbc.M107611200

Royce Mohan‡§, Shravan K. Chintala‡¶, Jae Chang Jung‡, Winston V. L. Villar, Frank McCabe, Laoti A. Russo, Yunhee Lee, Brendan E. McCarthy, Kurt R. Wollenberg, James V. Jester||, Min Wang**, Howard G. Welgus***‡, J. Michael Shipley§§, Robert M. Senior§§, and M. Elizabeth Fini¶¶

From the New England Eye Center, Tufts University School of Medicine, and the Tufts Center for Vision Research, Boston, Massachusetts 02111, the ||Department of Ophthalmology, University of Texas Southwestern Medical Center, Dallas, Texas 75390, and the **Division of Dermatology and §§Department of Medicine, Washington University School of Medicine at Barnes-Jewish Hospital, St. Louis, Missouri 63110

We studied the role of the matrix metalloproteinase gelatinase B (gelB; MMP-9) in epithelial regeneration using the gelB-deficient mouse. We report the novel finding that, in contrast to other MMPs expressed at the front of the advancing epithelial sheet in wounds of cornea, skin, or trachea, gelB acts to inhibit the rate of wound closure. We determined this to be due to control of cell replication, a novel capacity for MMPs not previously described. We also found that gelB delays the inflammatory response. Acceleration of these processes in gelB-deficient mice is correlated with a delay in signal transduction through Smad2, a transcription factor that inhibits cell proliferation, and in accumulation of epithelial-associated interleukin-1 α , a cytokine that inhibits Smad2 signaling and promotes the inflammatory response. GelB-deficient mice also reveal defects in remodeling of extracellular matrix at the epithelial basement membrane zone, in particular, failure to effectively remove the fibrin(ogen) provisional matrix. We conclude that gelB coordinates and effects multiple events involved in the process of epithelial regeneration.

Epithelial tissues surface all organs of the body exposed to the external environment, acting as a protective barrier. Unlike most organ stromal tissues, epithelia can regenerate completely following injury. Epithelial regeneration involves multiple distinct processes, including the concerted migration of

cells as a sheet to resurface the wound bed, mitosis to replace cell numbers, re-stratification of the sheet into a multilayered structure, and restoration of stable adhesive interaction with the underlying tissue stroma (1–6). These processes must be temporally coordinated with one another, and with the protective inflammatory response, which also occurs in response to injury. This is thought to involve an orderly progression and synergism of cytokines and growth factors within the wound environment (7–15). Despite many recent advances, mechanisms for integrating and orchestrating the multiple processes involved in epithelial regeneration are still poorly understood.

The matrix metalloproteinases (MMPs)¹ are a family of zinc endopeptidases that act as key effectors and regulators of tissue remodeling in vertebrates (16). Molecular substrates for the MMPs include all classes of extracellular matrix proteins and molecules that organize tissues such as the cadherins (17, 18). MMPs are also reactive against signaling molecules such as cytokines and growth factors, controlling their activity and bioavailability (18). While MMP activity is regulated at multiple levels, gene expression constitutes the major control mechanism (19). Induced expression of an array of MMPs occurs as part of the tissue response to injury (20, 21). Inappropriate expression or overexpression of MMPs contributes to the pathophysiology of diverse disorders occurring across all organ systems (22), including healing disorders (20, 23–25).

Gelatinase B (gelB; MMP-9) is an MMP that catalyzes cleavage of denatured collagens of all types and native basement membrane components (26, 16). In addition, recent work has identified fibrin(ogen) (27), α_1 -proteinase inhibitor (79), interleukin-1 (IL-1) (28, 29), and transforming growth factor- β (TGF- β) as gelB substrates (30). GelB is not expressed in the normal cornea, skin, or trachea; however, expression is induced (along with a number of other MMPs) in cells at the front of the migrating epithelial sheet as it begins to resurface the wound bed following injury (22, 31–33). Inflammatory cells infiltrating the wound bed also produce gelB (34, 35). GelB expression in the epithelium spreads progressively distal to the migrating front once wound resurfacing is complete and persists for several weeks thereafter (32, 36). The timing correlates with the period during which provisional wound matrix is resorbed and new structures for epithelial/stromal adhesion are assembled in the epithelial basement membrane zone (37). Overexpres-

* This work was supported by project grants AR42981 and EY12651 (to M. E. F.), EY07348 (to J. V. J.), and HL47328 (to R. M. S.), National Eye Institute Center Grant EY13078 (to M. E. F.), the Massachusetts Lions Eye Research Fund, Inc. (to M. E. F.), by an unrestricted grant from Research to Prevent Blindness (to M. E. F., and J. V. J.), the Alan A. and Edith L. Wolff Charitable Trust (to R. M. S.), and the New England Medical Center Hospitals Research Fund (to M. E. F.). The costs of publication of this article were defrayed in part by the payment of page charges. This article must therefore be hereby marked "advertisement" in accordance with 18 U.S.C. Section 1734 solely to indicate this fact.

‡ These authors contributed equally to the results of this work.

§ Present address: EntregMed, Inc., Rockville, MD 20850.

¶ Present address: Eye Research Institute, Oakland University, Rochester, MI 48309.

‡‡ Present address: Parke-Davis Pharmaceutical Research, Ann Arbor, MI 48103.

¶¶ Jules and Doris Stein Research to Prevent Blindness Professor. To whom correspondence should be addressed: New England Eye Center, Tufts University School of Medicine, 750 Washington St., Box 450, Boston, MA 02111. Tel.: 617-636-9027; Fax: 617-636-4594; E-mail: efini@lifespan.org.

¹ The abbreviations used are: MMP, matrix metalloproteinase; BrdU, bromodeoxyuridine; gelA, gelatinase A; gelB, gelatinase B; IL-1, interleukin 1; PRK, photorefractive keratectomy; TGF- β , transforming growth factor- β .

sion of *gelB* is associated with defective re-epithelialization and a reduction in adhesion complex integrity (23, 31). These data suggest that *gelB* plays a key role in the process of epithelial regeneration.

The corneal epithelium can be considered a prototype for a stratified epithelium similar to that surfacing skin, lung, and other organs. Moreover, the cornea offers an ideal model for evaluating mechanisms of tissue repair and regeneration because the avascularity of this organ reduces the number of interacting tissues. In this study we have investigated specific roles for *gelB* in regeneration of the corneal epithelium, utilizing a strain of mice made genetically deficient for *gelB*.

EXPERIMENTAL PROCEDURES

Mice and Surgical Procedures—*GelB*-deficient mice (*GelB*^{-/-}) were on the 129SvEv/CD-1 mixed background. A matched littermate control line (*GelB*^{+/+}) was on the same background (38). At intervals throughout this study, genotypes were verified by Southern blotting. Mice were used for experiments between 6 and 12 weeks of age; *gelB*-deficient mice were age-matched with littermate controls. Surgical procedures were performed on anesthetized mice according to approved institutional protocols. For corneal debridement surgery, the epithelium within an area demarcated by a 1.5-mm diameter trephine was removed to the basement membrane with the aid of an algebrush (Storz Ophthalmic). Photorefractive keratectomy (PRK) was performed on corneas using a Summit Apex Excimer Laser (Summit, Waltham, MA) on phototherapeutic settings. Tissue was ablated to a depth of 40–44 μm within a 2.0-mm diameter spot size using 160 pulses. To create a full thickness skin wound, hair was removed with a depilatory agent. Then the back skin was pulled up to form skin-to-skin double layers and a 6-mm punch biopsy sterilely used to create two identical full thickness wounds. The wounds were covered with transparent Op-Site dressing.

Quantification of Re-epithelialization Rate—Eyes were enucleated between 10 and 20 h after surgery and tethered to paraffin by pinning through the extraocular muscles. The remaining epithelial defects were delineated by application of Richardson's stain to the ocular surface. Images were projected at a fixed distance and the circumference of the area stained by blue dye was traced in pencil. The area was then quantified using NIH image software by an observer unaware of the mouse genotype.

To quantify healing in skin wounds, animals were anesthetized and then the outside perimeter was traced with a fine point marker onto a sterile slide directly applied to the wound site, after removing the old dressing and before applying a new one. The wound shape was traced immediately after surgery and every 2 days from the third day afterward. The image of the slide with the wound tracing was captured through a computerized video camera with Pax-it! Software (version 1.83, Imaging Systems for Science and Industry). The area of wound tracing on slide was quantified using computer image analysis software (Optimus).

Organ Culture—Eyes were enucleated immediately following surgery, tethered to paraffin beds in the individual wells of 24-well plates, and cultured in serum-free medium as described (32). For "rescue" experiments, purified recombinant human *gelB* proenzyme (Chemicon, Temecula, CA) was added to culture medium at the beginning of an experiment. In other experiments, organ cultures were treated with Ilomastat, a synthetic peptide hydroxamic acid analogue of the transition state of zinc metalloproteinases (39). A peptide analogue lacking the active hydroxamic acid group was used as a control (both agents from AMS Scientific, Pleasant Hill, CA).

Zymography—Epithelium from the repairing areas of corneas was debrided with a surgical scalpel, placed in 200 μl of ice-cold 200 Tris-HCl, pH 7.5, and pulverized with a Pellet Pestle (Kimble-Knotes, NJ). Insoluble material was removed by centrifugation at $14,000 \times g$ for 10 min at 4 °C. The soluble proteins were precipitated using cold acetone and protein concentration was determined with the Bio-Rad reagent. Gelatin zymography was performed according to our standard methods (31, 32).

Light Microscopy—Methacrylate cross-sections (6 μm) were stained with hematoxylin and eosin. Relative thickness of the corneal epithelial and stromal layers in *gelB*-deficient mice and normal mice was compared by examining 10 sections taken through the center of each cornea from 10 different mice of each strain. Measurements were made using a micrometer viewed in the light microscope field alongside the tissue section. Significance of differences between strains was assessed using the Student's *t* test.

Cryostat sections (6 μm) were processed for indirect immunofluorescent localization as described previously (31). The primary antibodies used were a rat polyclonal antibody against the inflammatory cell marker, mouse Mac-1 (CD11b/CD18 or $\alpha_M\beta_2$ integrin) (Chemicon, Temecula, CA), a mouse monoclonal antibody directed against human laminin-5 (40), a sheep polyclonal antiserum raised against human fibronectin (Chemicon, Temecula, CA), and a rabbit polyclonal antibody against mouse fibrin(ogen), which binds both the fibrinogen precursor and the proteolytically cleaved fibrin (41).

Confocal microscopy was performed on mouse corneas fixed with 1% paraformaldehyde in phosphate-buffered saline. Whole corneas were then stained *en bloc* with rhodamine-conjugated phalloidin (Molecular Probes, Eugene, OR) to identify actin filaments. Corneas were mounted epithelial side down onto 25- μm thick, 60-mm diameter mylar Petri dishes (Bachofar, Hamburg, Germany) and scanned using a confocal microscope (Confocal Laser Scanning Microscopy, Leica, Deerfield, IL) equipped with a Leica Fluorovert microscope, argon/krypton laser and 568/590 excitation/detection filters. Three-dimensional data sets were collected and transferred to a Silicon Graphics work station (Personal Iris 4D-35G), and maximum intensity volume renderings were made using the ANALYZE software program (Mayo Medical Adventure Inc., Rochester, MN).

BrdU Labeling and Detection—Central corneal debridement (1.5-mm) wounds were made in the right eyes of the mice and allowed to heal for 16 h *in vivo*. Two hours before the mice were sacrificed, BrdU (Sigma) dissolved in phosphate-buffered saline was injected subcutaneously in the dorsal subscapular region at 100 $\mu\text{g/g}$ body weight. Mice were sacrificed and the eyes removed immediately and frozen for cryostat sectioning. Cross-sections were immunohistochemically stained with a monoclonal antibody against BrdU (Becton Dickinson, San Jose, CA). The primary antibody was detected by avidin-biotin complex immunoperoxidase technique using an ABC Elite Kit (Vector Laboratories, Burlingame, CA) following the manufacturer's directions. Color was developed with 3',3'-diaminobenzidine peroxidase substrate (Sigma).

Western Blotting—Eyes were frozen immediately after the mice were sacrificed by immersion in liquid nitrogen to prevent Smad activation during sample preparations. The entire corneal epithelium was then removed by gentle scraping with a scalpel. The pooled tissues from 10 eyes were lysed in a buffer containing 50 mM Tris-HCl, pH 7.4, 1% Nonidet P-40, 0.25% sodium deoxycholate, 150 mM NaCl, 1 mM EGTA, 1 mM phenylmethylsulfonyl fluoride, 1 $\mu\text{g/ml}$ each aprotinin, leupeptin, pepstatin, 1 mM Na_3VO_4 , 10 mM NaF. Equal amounts of protein (10 $\mu\text{g/sample}$) were separated by 10% SDS-PAGE, transferred onto polyvinylidene difluoride membranes and probed with specific primary antibody reagents. Immunodetection of primary antibody binding was accomplished by incubation with horseradish peroxidase-conjugated secondary antibody followed by chemiluminescence (PerkinElmer Life Sciences) and exposure to x-ray film. Rabbit anti-Smad3 and anti-phospho-Smad2 were purchased from Upstate Biotechnology (Lake Placid, NY), and monoclonal anti-Smad2 (clone 18) was purchased from Transduction Laboratories (San Diego, CA). A goat polyclonal antibody raised against recombinant mouse IL-1 α (catalog number AF-400-NA) was purchased from R & D Systems (Minneapolis, MN). Information in the company catalogue states that this antibody was selected for its ability to neutralize the biological activity of recombinant mouse IL-1 α . Based on direct enzyme-linked immunosorbent assay and Western blot results, this antibody showed less than 10% cross-reactivity with recombinant human IL-1 α . Additionally, indirect enzyme-linked immunosorbent assays this antibody showed no cross-reactivity with other cytokines tested.

RESULTS

***GelB*-deficient Mice Have Normal Corneas**—Mice homozygous for a targeted mutation that inactivates the gene for *gelB* show delayed growth of long bones due to impaired vascularization of the growth plate, but ultimately they attain normal adulthood (38). Routine gross examination of adult eyes revealed no obvious anatomical differences between *gelB*-deficient homozygotes and their normal counterparts. Eyes of the *gelB*-deficient mice were of normal size and lenses were clear. Corneas were clear and avascular, with no evidence of malformation or inflammation by gross or histological analysis (data not shown). No statistically significant difference was observed between strains in stromal or epithelial layer thickness, or in number of epithelial layers (data not shown). These observa-

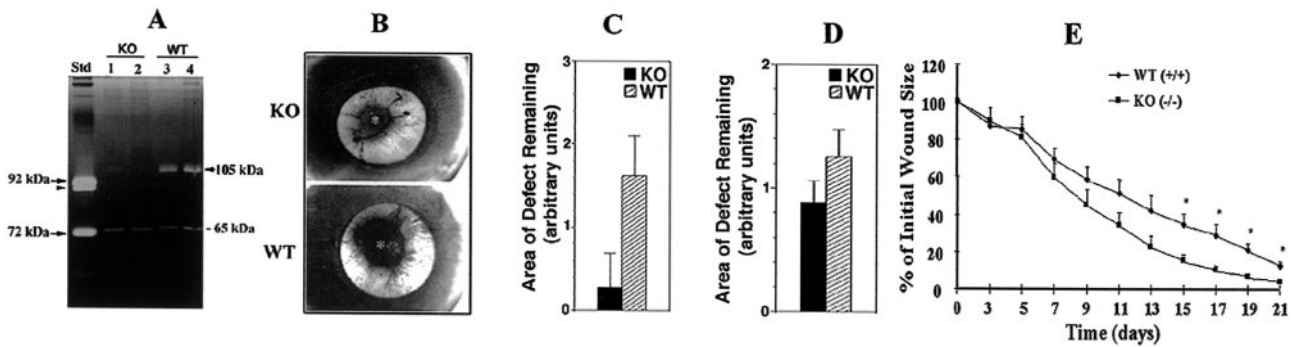


FIG. 1. Increased rate of corneal re-epithelialization in gelB-deficient mice. Epithelial debridement or PRK surgery was performed on normal “wild-type” (WT) and gelB-deficient “knock-out” (KO) mice. The *graphs* represent the relative mean areas of remaining epithelial defects at the indicated time point after surgery. Statistical analysis was performed using the Student’s *t* test. **A**, gelatin zymographic analysis of extracts from epithelium collected 18 h after debridement surgery. *Lanes 1 and 2 and lanes 3 and 4* are duplicate samples. A rabbit fibroblast standard (*Std*) was co-electrophoresed with the mouse samples. Mouse progelB migrates with an apparent M_r of 105,000 as compared with the rabbit homolog of 92,000. The absence of the 105,000 zymogram band is noted in the extracts from the gelB-deficient mouse corneas. The *arrowhead* indicates the glycosylated form of 92-kDa gelB. The *arrow* indicates mouse pro-gelA, which migrates with an apparent M_r of 65,000. **B**, representative photographic images of stained corneas from gelB-deficient and normal mice sacrificed at the 15-h time point after epithelial debridement surgery. The *asterisks* mark the central area of the irregularly shaped wound perimeter, defined by the *dark stain*. **C**, the *graph* represents data obtained from experiments similar to that in **B** where mice were sacrificed after 20 h following epithelial debridement surgery; $p < 0.002$ ($n = 10$). This difference was reproducible in a subsequent reiteration of the experiment. **D**, the *graph* represents the 20-h time point after PRK surgery; $p < 0.01$ ($n = 12$). **E**, the *graph* depicts the rate of wound closure for 6-mm full-thickness punch biopsies in skin. The remaining wound size was quantified over a period of 21 days and represented as the percent of the initial wound size. Asterisk (*) indicates < 0.01 ($n = 8$ or 9 for each experimental group).

tions indicate that a deficiency of gelB does not affect the formation and maintenance of normal corneal structure.

Increased Rate of Corneal Re-epithelialization in GelB-deficient Mice—To investigate the effects of gelB deficiency on regeneration of the corneal epithelium following injury, we used an epithelial debridement model (42, 32) adapted for the mouse in which the epithelium is surgically removed to the level of the basement membrane within a circular region of 1.5-mm diameter. We collected epithelial tissue from the repairing portions of normal and gelB-deficient corneas at a time when wounds were partially closed, and analyzed tissue extracts by gelatin zymography (Fig. 1A). A gelatinase of a size appropriate to be the gelB proenzyme was detectable in extracts derived from littermate control mice, but was absent from extracts derived from gelB-deficient mice. In contrast, a gelatinase of the size appropriate to be the gelatinase A (gelA; MMP-2) proenzyme was detectable in extracts from both gelB-deficient mice and their normal counterparts. The intensity of the gelA band was essentially the same in both mouse lines, indicating that gelB deficiency does not result in compensatory up-regulation of this related enzyme.

A time course experiment was performed over the period of wound closure, and the rate of re-epithelialization was compared between gelB-deficient mice and normal littermate controls. Fig. 1B shows representative images of the remaining epithelial defects at a time when wounds were partially closed. No difference was observed in the quality of re-epithelialization between mouse strains. Corneas from both gelB KO mice and their normal counterparts re-epithelialized without incident, with no gross evidence of inflammation. In contrast, the rate of re-epithelialization was faster in the gelB-deficient mice. This difference was apparent as early as 10 h after surgery, and was highly significant by 20 h (Fig. 1C). All corneas from both mouse strains remained avascular throughout this experiment, indicating that cytokines or other factors contributed by the vasculature could not cause the differing re-epithelialization rates.

The substrate on which the epithelium migrates could influence the rate of wound resurfacing. Therefore, we repeated the experiment described above using a PRK model in which a laser is used to ablate superficial corneal tissue removing the

epithelium, the basement membrane, and a portion of the anterior stroma. To resurface this type of wound, the epithelial sheet migrates across stromal collagen fibrils. Again, no difference in the quality of healing was observed between gelB-deficient mice and their normal counterparts; however, re-epithelialization was still significantly faster in the gelB-deficient mice (Fig. 1D).

To learn whether faster wound closure generalizes to other organs, we examined the rate of healing of an excisional wound in the skin (Fig. 1E). As in cornea, wound closure in skin was found to occur significantly more rapidly in gelB-deficient mice than in their normal control counterparts. These results indicate that the findings in cornea are not tissue-specific.

The GelB-deficient Re-epithelialization Phenotype Is Due to a Direct Loss-of-function in the Eye and Is Different from the Phenotype Resulting from Broad Spectrum MMP Deficiency—To differentiate between systemic and local factors in the gelB-deficient phenotype, we repeated the surgical debridement experiment, but eyes were enucleated following surgery and placed in organ culture for healing. The difference in the re-epithelialization rate between normal and gelB-deficient mice was less than when re-epithelialization occurred in the mouse *in situ*, but was still significant at 15 h ($p < 0.002$; $n = 10$; data not shown) and 20 h after surgery (Fig. 2A). These data indicate that at least some of the effects of gelB deficiency are attributable to local factors.

To provide evidence that the corneal re-epithelialization phenotype in the gelB-deficient mice is due to a direct loss-of-function, we attempted a rescue experiment by adding purified gelB protein to the corneas of gelB-deficient mice undergoing re-epithelialization in organ culture. GelB was added in the latent proenzyme form, because this is the form that predominates in re-epithelializing debridement wounds (see Fig. 1A). Our expectation was that the exogenously added proenzyme would be converted to an active form through the same extracellular mechanisms utilized for activation of endogenously produced enzyme during wound repair. At 1 $\mu\text{g/ml}$ of exogenously added gelB proenzyme, the retardation of re-epithelialization rate was significant (Fig. 2B). In other words, exogenous addition of gelB returned the rate of wound re-epithelialization in the gelB-deficient mouse back toward

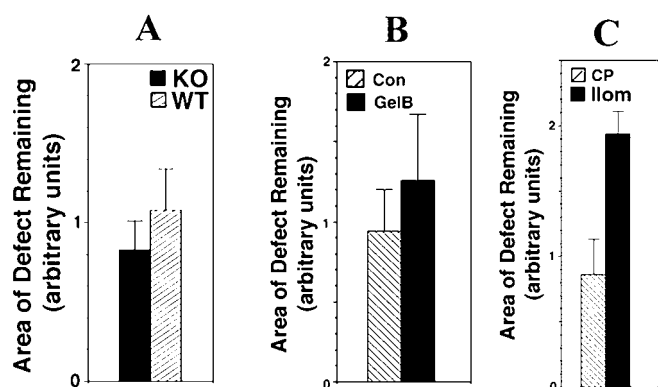


FIG. 2. The *gelB*-deficient re-epithelialization phenotype is due to a direct loss-of-function in the eye, and is different from the phenotype resulting from broad-spectrum MMP deficiency. Epithelial debridement surgery was performed on groups of normal wild-type (*WT*) and *gelB*-deficient knock-out (*KO*) mice and then the animals were sacrificed and the eyes were removed to organ culture for re-epithelialization *in vitro*. The graphs represent areas of remaining epithelial defects at the indicated time point after surgery. Statistical significance was determined using the Student's *t* test. *A*, organ-cultured corneas at the 20-h time point; $p < 0.02$; $n = 8$ for each group. *B*, organ-cultured corneas from *gelB*-deficient mice were treated with recombinant human pro-*gelB* for 18 h. $p < 0.003$. $n = 6$ for each group. *C*, organ-cultured corneas from *gelB*-deficient mice were treated with $1 \mu\text{M}$ ilomastat (*Ilom*) or control peptide (*CP*) for 18 h. $p < 0.017$. $n = 6$ for each group.

normal, consistent with rescue of the deficiency phenotype. These data support the conclusion that the *gelB*-deficient re-epithelialization phenotype results from a direct loss-of-function due to inactivation of the gene for *gelB*.

Inhibition of broad-spectrum or specific MMP activity has been reported to inhibit epithelial cell migration in culture (21, 33, 43) and to retard re-epithelialization of skin wounds in organ culture and *in vivo* (21, 44). To learn whether this is also true in our corneal model, we examined the effects of Ilomastat, a broad spectrum MMP inhibitor (39, 45) on re-epithelialization in normal mice. While the K_i for gelatinases determined in test tube assay is 0.4 nM , inhibition of MMPs in tissues requires much higher concentrations; we used the dose range determined to be effective by Chin and Werb (46) in their studies with a mandibular organ culture system. At an ilomastat dose of $1 \mu\text{M}$, the rate of corneal re-epithelialization was significantly retarded in comparison to controls treated with the same dose of an inactive analogue lacking the hydroxamic acid group (Fig. 2C). These data are consistent with a requirement for MMP activity in corneal re-epithelialization, and suggest that *gelB* must be playing a different role than other MMPs in this process.

Earlier Inflammatory Cell Infiltration, Increased Deposition of Provisional Matrix, and Enhanced Rate of Epithelial Cell Replacement in *GelB*-deficient Mice—Tangential optical sectioning by confocal microscopy on corneal whole mounts stained with rhodamine-phalloidin revealed no differences between *gelB*-deficient mice and their normal counterparts in the overall appearance, or in organization of the actin filaments, in cells at the advancing epithelial front (Fig. 3, *Confocal*, *arrows*). However, in the course of these experiments we observed the presence of inflammatory cells in the wound bed of *gelB*-deficient mice (Fig. 3, *Confocal*, $-/-$, *arrowhead*), that were not seen in their normal counterparts (Fig. 3, *Confocal*, $+/+$, *arrowhead*). Absence of *gelB* does not appear to alter the capacity of inflammatory cells to respond to a chemotactic stimulus, extravasate from blood vessels, or accumulate in tissues (47). However, a deficiency in *gelB* was shown to delay the resolution of the contact hypersensitivity response in skin (48). A

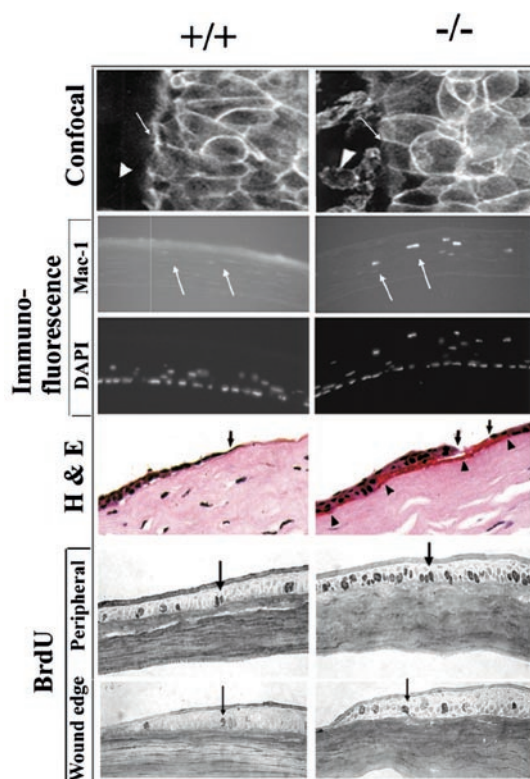


FIG. 3. Earlier inflammatory cell infiltration, increased deposition of provisional matrix, and enhanced rate of epithelial cell replacement in *gelB*-deficient mice. Epithelial debridement surgery was performed on the corneas of normal ($+/+$) and *gelB*-deficient ($-/-$) mice, and corneas were collected for analysis just prior to wound closure (16–18 h). *Confocal*, tangential optical sections by confocal microscopy through the epithelium of rhodamine-phalloidin-stained corneal whole mounts, taken 18 h after surgery. *Arrows* indicate the migrating epithelial front. The *arrowhead* indicates invading inflammatory cells in the wound bed. *Immunofluorescence*, frozen cross-sections of corneas taken 16 h after surgery and stained by indirect immunofluorescence using the inflammatory cell marker Mac-1. Shown is the central portion of cornea which is still not re-epithelialized at this time point. *Arrowheads* indicate positively stained cells. Corneas were counterstained with Hoechst322 dye (*DAPI*) which binds the nuclear DNA of all cells. *H & E*, corneal cross-sections taken 18 h after surgery were stained with hematoxylin and eosin and visualized by light microscopy. The presence of eosinophilic deposits in the *gelB*-deficient cornea is indicated by the *arrowheads*. The leading edge of the migrating epithelium is indicated by the *arrows*. *BrdU*, corneal cross-sections stained with BrdU antibody to visualize cells undergoing DNA synthesis. *Arrows* indicate positively stained cells.

systematic investigation of inflammatory cell infiltration by immunofluorescent microscopy on cross-sections revealed consistent staining with the Mac-1 marker in corneas from *gelB*-deficient mice examined prior to epithelial closure (Fig. 3, *Immunofluorescence*, *Mac-1*, $-/-$, *arrow*), while no staining was observed in normal mice (Fig. 3, *Immunofluorescence*, *Mac-1*, $+/+$, *arrow*). However, shortly after wound closure (24 h post-surgery), corneas from all normal mice stained for the Mac-1 marker, and the amount of staining appeared only slightly less than in the *gelB*-deficient mice (data not shown).

In histologically stained cross-sections, the migrating epithelial sheet appeared as a monolayer in normal mice but was multilayered in the *gelB*-deficient mice (Fig. 3, *H & E*, *arrows*). In addition, an eosinophilic deposit was apparent in the wound bed and below the migrating epithelium in some *gelB*-deficient mice that was not observed in their normal counterparts (Fig. 3, *H & E*, *arrowheads*). This seemed likely to represent an accumulation of provisional wound matrix and is discussed further below. Bromodeoxyuridine (BrdU) labeling was per-

formed on corneal cross-sections to identify cells undergoing DNA synthesis (Fig. 3, *BrdU*). It is known that epithelial injury stimulates proliferation of cells distal to the wound edge, while the rate of proliferation decreases in cells at the migratory front (49, 50). Consistent with this, *BrdU*-labeled cells from corneas of both normal and *gelB*-deficient mice were concentrated in the peripheral epithelium, with fewer labeled cells localized to the migratory front (central). In both locations, however, the number of labeled cells was clearly greater in the *gelB*-deficient mice. These data provide evidence that *gelB* deficiency enhances the rate of epithelial resurfacing of corneal wounds by increasing the pressure exerted as a result of cell proliferation.

***GelB* Deficiency Is Associated with a Delay in *Smad2* Signaling and an Increase in Cell-associated *IL-1 α* in the Regenerating Corneal Epithelium**—*GelB* can cleave a variety of molecules involved in cell signaling (18), and thus *gelB* deficiency might alter the net signaling information received at the cell surface and cause the changes observed above. A deficiency in the transcription factor *Smad3* was recently shown to enhance the rate of cutaneous wound re-epithelialization by increasing cell proliferation (51), similar to our findings here on the *gelB*-deficient phenotype. Both *Smad3* and its closely related homologue, *Smad2*, translocate from the cytoplasm to the nucleus once phosphorylated in response to signals received at the cell surface (52). Immunohistochemical staining of cross-sections through corneas of normal mice revealed that *Smad3* undergoes translocation into nuclei throughout the regenerating corneal epithelium following debridement surgery (Fig. 4A). Western blotting revealed that *Smad2* and *Smad3* activity was clearly increased in the regenerating epithelium of normal mice (Fig. 4B, +/+). For *Smad2*, increased activity was demonstrated by comparison of the levels of total *Smad2* and phosphorylated *Smad2*. For *Smad3*, reprobing of the same Western blot revealed a new immunoreactive band of slower electrophoretic mobility in regenerating epithelium, consistent with phosphorylation. These findings are consistent with a role for *Smad2* and *Smad3* in controlling the rate of epithelial cell proliferation.

Western blot analysis of the regenerating epithelium from *gelB*-deficient mice showed the same overall changes in *Smad2* and *Smad3* as the normal mice (Fig. 4B, -/-). The amount of the putative active form of *Smad3* was similar in the *gelB*-deficient mice and their normal counterparts. However, activation of *Smad2* was clearly delayed in the *gelB*-deficient mice; an increase was not observed until the 16-h time point, and this increase was less than that seen in normal mice.

Since the cornea is avascular, the corneal wound is devoid of platelets, a major source of TGF- β and other cytokine mediators of wound repair. However, the corneal epithelium synthesizes TGF- β , IL-1, and other cytokines (53–55) and is thought to substitute for platelets in controlling the repair process (56). Western blot analysis of cell extracts from regenerating epithelium was performed to compare the levels of cell-associated TGF- β and IL-1 at the 8-h time point (Fig. 4C). No difference in the levels of the major TGF- β isoform produced by corneal epithelium (54) could be detected between *gelB*-deficient mice and their normal counterparts (data not shown). However, the amount of the major corneal IL-1 form, IL-1 α (53), was considerably increased in the *gelB*-deficient mice (Fig. 4C). Immunofluorescent localization analysis confirmed this increase, with greater IL-1 α observed within cells throughout the migrating epithelium (data not shown). Since IL-1 α is an antagonist of TGF- β signaling (76, 77), these data are consistent with the reduction in *Smad2* signaling in *gelB*-deficient mice. Since IL-1 α is an inflammatory cytokine, itself chemotactic for leu-

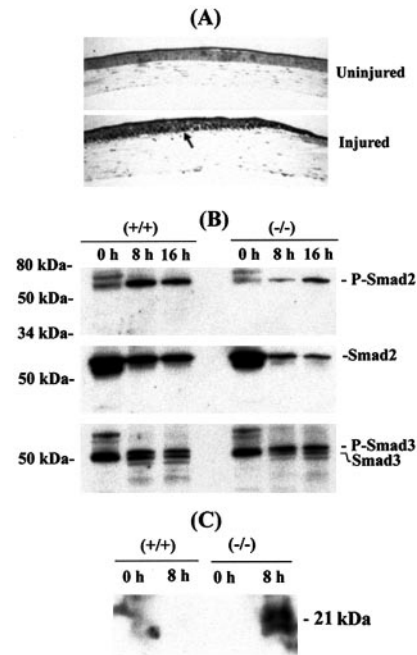


FIG. 4. *GelB* deficiency is associated with a delay in *Smad2* signaling and an increase in epithelial cell-associated IL-1 α in the regenerating corneal epithelium. A, cross-sections through the uninjured cornea of from normal wild-type (+/+) mice and through corneas at the 16-h time point after debridement surgery. Sections were immunostained with antibody to *Smad3*. Arrows indicate translocation of *Smad3* protein into nuclei in the migrating epithelium. B, Western blot of cell lysates from uninjured corneal epithelium (0 h), and from the migrating epithelium of corneas, 8 h (8 h) and 16 h (16 h) after epithelial abrasion surgery. Lanes were loaded with equal amounts of protein as determined by BCA assay, and equality of loading was confirmed by Coomassie Blue staining on a parallel set of lanes. The blot was probed with antibodies against *Smad3*, *Smad2*, and with an antibody specific for the phosphorylated form of *Smad2* (*pSmad2*). Immunoreactive proteins are indicated by an arrow. The putative phosphorylated *Smad3* isoform (*pSmad3*) is also indicated by an arrow. C, Western blot of cell lysates from uninjured corneal epithelium (0 h), and from migrating epithelium collected 8 h (8 h) after epithelial abrasion surgery. The blot was probed with an antibody to IL-1 α . The immunoreactive protein is indicated with an arrow.

kocytes (82), the increased levels of IL-1 α are also consistent with the earlier onset of inflammatory cell infiltration.

Impaired Basement Membrane Zone Remodeling and Accumulation of Provisional Matrix After Injury in *GelB*-deficient Mice Compromises Corneal Transparency—In normal skin or corneal wounds, a provisional extracellular matrix composed of fibrin(ogen) and fibronectin is deposited in the wound bed from the serum or tear film, and provides a substrate for cell attachment and migration (57–62). This matrix is resorbed once the wound is resurfaced and is replaced by new epithelial/stromal anchoring complexes (37, 64). The eosinophilic deposits apparent in the wound bed of *gelB*-deficient mice (see Fig. 3, *H & E*), suggested that remodeling in the basement membrane zone might be defective. We investigated this hypothesis by immunofluorescence analysis (Fig. 5A). In the unwounded areas of both *gelB*-deficient and normal corneas that had been healing for 6 days following PRK, the anchoring fibril component laminin 5 was present as a thin linear band between the epithelium and the stroma, and there was no staining for fibronectin or fibrinogen. This staining pattern had returned in the wound bed of the normal control mice, consistent with the timing of basement membrane zone remodeling observed in previous studies (32, 60). In contrast, the immunoreactive band of laminin-5 was thick and uneven in the wound bed of *gelB*-deficient corneas at the 6-day time point, and small amounts of fibronectin

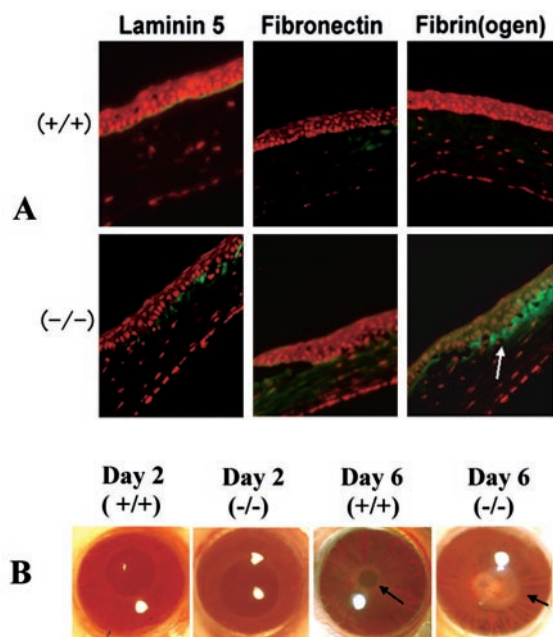


FIG. 5. Impaired basement membrane zone remodeling and accumulation of provisional matrix in *gelB*-deficient mice compromises corneal transparency. *A*, cross-sections from corneas taken from normal (+/+) and *gelB*-deficient mice (-/-) 6 days after PRK. Indirect immunofluorescence microscopy was used to identify laminin-5, fibronectin, and fibrin(ogen). The *arrow* indicates immunoreactive fibrin(ogen) which accumulates in eyes from *gelB*-deficient mice. *B*, eyes of normal mice (+/+) and *gelB*-deficient mice (-/-) were photographed 2 or 6 days after PRK. *Arrows* indicate corneal opacities.

tin were present. Most strikingly, a large fibrinogen deposit was apparent in the wound bed of the *gelB*-deficient mice. These results indicate impaired resorption of provisional matrix and re-establishment of epithelial/stromal adhesion complexes in *gelB*-deficient mice.

Defective remodeling at the epithelial basement membrane zone would have undesirable consequences for long-term health of the epithelium and could compromise organ function. In cornea, defective remodeling might interfere with the transparency necessary for transmittal of light to the retina of the eye. To investigate this hypothesis, we followed wound healing after PRK over a 2-week time course experiment. Representative results are shown in Fig. 5*B*, and data are summarized in Table I. Two days post-PRK, re-epithelialization was complete, and the corneas of normal mice were completely transparent. A minimal amount of clouding or “haze” was observed in some of the *gelB*-deficient mice at this time point, at a level too low to be recorded by photography. By 6 days post-PRK, some of the corneas from normal mice exhibited well defined, diffuse haze. However, many of the *gelB*-deficient mice exhibited haze, of a degree to obstruct iris detail. By day 14, haze was mostly resolved in the normal mice, but overall haze was increased in the *gelB*-deficient mice. This clouding is very similar to that reported after corneal wound healing in the plasminogen-deficient mouse (41). At no point was there any evidence of neovascularization of the avascular corneas at any time point in any experimental animal; thus the excessive material deposited could not have been due to vascular differences. These results suggest that defective resorption of provisional matrix and remodeling at the basement membrane zone due to the absence of *gelB* causes corneal clouding.

DISCUSSION

MMP expression is induced in cells at the migrating epithelial front in healing wounds of cornea, skin, or lung, and the

TABLE I
*Comparison of corneal clarity in repairing corneas of *gelB*-deficient mice and their normal counterparts following photorefractive keratectomy*

Corneal clarity was graded by an observer unaware of the mouse genotype. Grade 0 indicate complete clarity with no sign of haze, grade 0.5 indicate mild haze, grade 1 indicates well defined diffuse haze, grade 2 indicates obstruction of iris detail, and grade 3 indicate complete obstruction of the anterior chamber and iris. The number in parentheses indicates the number of animals with observable haze/the number of total animals examined. $p \leq 0.001$ (comparing normal and *gelB*-deficient mice using the non-parametric Mann-Whitney U test).

Mouse strain	Haze grading		
	Day 2	Day 6	Day 14
Normal	0 (0/12)	0 (0/12)	0 (0/12)
<i>GelB</i> -deficient	0.5 (2/12)	1 (10/12)	2 (8/12)

combined evidence to date (including data presented here) has supported the hypothesis that MMPs function to promote epithelial resurfacing by stimulating cell migration (22, 43, 44). Moreover, there is evidence to support this role specifically for *gelB* (33, 65). MMPs, including *gelB*, have further been implicated in a larger way in the process of cell migration involving many other tissues. Again, the roles identified for MMPs have been consistently facilitative and include the clearing of extracellular matrix to break down physical barriers, modulation of adhesive interactions with the extracellular matrix to release cells and to provide traction for their movement, and exposure of signals necessary to effect motor function and provide chemoattraction (18). The results reported here reveal that, while *gelB* may be involved in epithelial sheet migration, it is clearly not essential for this process in the normal *in vivo* situation. In fact, we show that a deficiency in *gelB* actually accelerates the rate of normal wound resurfacing. This is the first time that an MMP has been shown to exert negative control over cell migration. We show that *gelB* does this by inhibiting cell replication in the migrating epithelial sheet. This is a novel role for an MMP, not previously identified.

Peripheral to the main purpose of the current study, we made the new and significant observation that Smad2/Smad3 signaling is activated in the regenerating corneal epithelium. Smad signaling inhibits cell replication (52, 66), and thus Smad activation seems at first counterproductive to the requirement for cell replacement in epithelial regeneration. This can be understood, however, when we take into account that epithelial regeneration involves several other distinct processes, including resurfacing of the wound bed, re-stratification into a multilayered structure, and restoration of stable adhesive interaction with the underlying stroma. Each of these processes is associated with a withdrawal from the cell cycle (49, 50), and it is here that Smad activation may play a role.

Significantly, we found a specific delay in activation of Smad2 but not Smad3 in the *gelB*-deficient mice. Smad2 and Smad3 are the major downstream effectors of TGF- β signaling; however, there is accumulating evidence to suggest that these proteins are functionally different (52, 66). While activity of both are stimulated by TGF- β signaling, they can be differentially regulated as a result of cross-talk among signaling pathways activated by other extracellular ligands. The IL-1 signaling pathway interacts with the Smad signaling pathway in this way; therefore the premature increase in IL-1 α levels observed in this study may translate into a specific delay in Smad-2 signaling (76–78, 80–81). *GelB* is selectively active against the IL-1 β isoform, although a minor capacity to cleave IL-1 α could still translate into a major effect in a specific microenvironment *in situ*. However, *GelB* could alter the accumulation of IL-1 α by

any number of indirect mechanisms including degradation of a proteinase that degrades IL-1 α or degradation of a cytokine that stimulates expression of IL-1 α by epithelial cells (for example, see Refs. 27, 30, and 79). Therefore, it seems likely that the levels of IL-1 α may be controlled by gelB through the enzymes action against multiple substrate.

Our findings also indicate that gelB controls the timing of the inflammatory response in the repairing cornea. Again, this may be attributed to premature accumulation of IL-1 α , which is a chemoattractant for leukocytes (63). In a similar vein, an alteration in cytokine profiles was identified as the mechanism for delayed inflammatory cell resolution in a cutaneous chemical hypersensitivity model applied to the gelB-deficient mice (48). The joint regulation of wound closure and inflammation by controlling the levels of a single cytokine, IL-1 α , could serve to coordinate the timing of these two processes.

Our work shows that gelB alters the "instructions" that cells receive from the microenvironment, thus mediating very specific alterations in intracellular signaling pathways, and fine tuning of the regenerative process. Not only must cell replication be temporal-coordinated with the other processes involved in epithelial regeneration, but also spatially coordinated. Thus, the progressive change in expression pattern of gelB during epithelial regeneration may be a key factor in its ability to perform a fine tuning function (31, 32, 36). Expression at the leading edge of the migrating corneal epithelium may serve to coordinate what is happening at the migrating front with the cell replication that occurs distal to the front. Later, when the wound is closed, expression across the entire regenerating epithelium may be important for the complete resorption of provisional matrix and restoration of normal epithelial/stromal adhesion.

The accumulation of fibrin(ogen) in the wound bed was a striking aspect of the gelB-deficient phenotype found in this study and indicates that gelB acts not only to coordinate but also to effect events involved in epithelial regeneration. Recent work has shown that pericellular fibrinolysis by migrating endothelial cells is MMP-mediated (67). As this article was in preparation, it was reported that fibrin(ogen) accumulation occurs in the gelB-deficient mouse in a kidney disease model and that gelB can cleave purified fibrinogen in a test tube assay (27). Thus gelB may act directly on the temporary fibrin(ogen) scaffolding. GelB may also effect fibrin(ogen) removal indirectly, for example, by its ability to proteolytically activate plasminogen activator, or by its ability to proteolytically inactivate inhibitors of the plasmin-plasminogen activator cascade, such as PAI-1 (26).

Excessive deposition of fibrin(ogen) due to the absence of gelB appeared to be a major reason for corneal clouding. Corneal clouding or haze is an undesirable side effect of the wound healing process after corrective PRK (68) and can be visually debilitating in 1% of human patients (69–73). Excessive fibrin(ogen) deposition was also associated with defective restoration of stable adhesive interactions with the corneal stroma. Again, this suggests parallels to human pathology. Chronic wounds of skin and cornea are typically characterized by a hyperplastic epithelium (20, 23, 31, 74), which fails to migrate properly across the wound bed or form proper attachments to the underlying stroma. This leads to persistent or recurrent epithelial defects. While fibrin accumulating in acute wounds is removed within days, it persists in chronic cutaneous wounds (75, 74). It has been suggested that excessive fibrin deposition may contribute to pathophysiology, by "trapping" of cytokines controlling epithelial cell dynamics, and by physically interfering with the restoration of stable epithelial/stromal adhesion.

Taking the findings of this study into consideration with the

results of previous work, we conclude that a balance of gelB activity must be struck for health of epithelial tissues; too little activity or too much activity can both lead to pathology. However, it appears that timing and location of gelB expression in the microenvironment is also critical to the overall picture of health or pathology. Understanding the mechanisms for controlling the pattern of gelB expression will be a future challenge.

Acknowledgment—We thank Dr. Jay L. Degen (Children's Hospital Research Foundation, Cincinnati, OH) for his gift of fibrin(ogen) antibody.

REFERENCES

- Woodley, D. T., O'Keefe, E. J., and Prunieras, M. (1985) *J. Am. Acad. Dermatol.* **12**, 420–433
- Guo, M., and Grinnell, F. (1989) *J. Invest. Dermatol.* **93**, 372–378
- Fuchs, E. (1990) *J. Cell Biol.* **111**, 2807–2814
- Watt, F. M., Hudson, D. L., Lamb, A. G., Bolsover, S. R., Silver, R. A., Aitchison, M. J., and Whitaker, M. (1991) *J. Cell Sci.* **99**, 397–405
- Phillips, T. J., and Gilchrist, B. A. (1992) *Epithelial Cell Biol.* **1**, 39–46
- Singer, A. J., and Clark, R. A. (1999) *N. Engl. J. Med.* **341**, 738–746
- Schultz, G., Khaw, P. T., Oxford, K., MacCauley, S., Van Setten, G., and Chegini, N. (1994) *Eye* **8**, 184–187
- Gipson, I. K., and Inatomi, T. (1995) *Curr. Opin. Ophthalmol.* **6**, 3–10
- Pierce, G. F., and Mustoe, T. A. (1995) *Annu. Rev. Med.* **46**, 467–481
- Schaffer, C. J., and Nanney, L. B. (1996) *Int. Rev. Cytol.* **169**, 151–181
- Werner, S. (1998) *Cytokine Growth Factor Rev.* **9**, 153–165
- Davidson, J. M., Whitsitt, J. S., Pennington, B., Ballas, C. B., Eming, S., and Benn, S. I. (1999) *Curr. Top. Pathol.* **93**, 111–121
- Wilson, A. J., Byron, K., and Gibson, P. R. (1999) *Clin. Sci. (Colch.)* **97**, 385–390
- Zieske, J. D., Takahashi, H., Hutcheon, A. E., and Dalbone, A. C. (2000) *Invest. Ophthalmol. Vis. Sci.* **41**, 1346–1355
- Hunt, T. K., Hopf, H., and Hussain, Z. (2000) *Adv. Skin Wound Care* **13**, 6–11
- Woessner, J. F. (1998) in *Matrix Metalloproteinases* (Parks, W. C., and Mecham, R. P., eds) pp. 1–14, Academic Press, San Diego
- Lochter, A., Galosy, S., Muschler, J., Freedman, N., Werb, Z., and Bissell, M. J. (1997) *J. Cell Biol.* **139**, 1861–1872
- Vu, T. H., and Werb, Z. (2000) *Genes Dev.* **14**, 2123–2133
- Fini, M. E., Cook, J. R., Mohan, R., and Brinckerhoff, C. E. (1998) in *Matrix Metalloproteinases* (Parks, W. C., and Mecham, R. P., eds) pp. 299–356, Academic Press, San Diego
- Fini, M. E., Cook, J. R., and Mohan, R. (1998) *Arch. Dermatol. Res.* **290**, (suppl.) S12–23
- Pilcher, B. K., Dumin, J. A., Sudbeck, B. D., Krane, S. M., Welgus, H. G., and Parks, W. C. (1997) *J. Cell Biol.* **137**, 1445–1457
- Parks, W. C., and Mecham, R. P. (eds) (1998) *Matrix Metalloproteinases*, Academic Press, San Diego
- Fini, M. E., Parks, W. C., Rimehart, W. B., Girard, M. T., Matsubara, M., Cook, J. R., West-Mays, J. A., Sadow, P. M., Burgeson, R. E., Jeffrey, J. J., Raizman, M. B., Krueger, R. R., and Zieske, J. D. (1996) *Am. J. Pathol.* **149**, 1287–1302
- Ravanti, L., and Kahari, V. (2000) *Int. J. Mol. Med.* **6**, 391–407
- Parks, W. C. (1999) *Wound Repair Regen.* **7**, 423–432
- Vu, T. H., and Werb, Z. (1998) in *Gelatinase B: Structure, Regulation, and Function, Matrix Metalloproteinases* (Parks, W. C., and Mecham, R. P., eds) Academic Press, San Diego
- Lelongt, B., Bengatta, S., Delauche, M., Lund, L. R., Werb, Z., and Ronco, P. M. (2001) *J. Exp. Med.* **193**, 793–802
- Schonbeck, U., Mach, F., and Libby, P. (1998) *J. Immunol.* **161**, 3340–3346
- Ito, A., Mukaiyama, A., Itoh, Y., Nagase, H., Thogersen, I. B., Engchild, J. J., Sasaguri, Y., and Mori, Y. (1996) *J. Biol. Chem.* **271**, 14657–14660
- Yu, Q., and Stamenkovic, I. (2000) *Genes Dev.* **14**, 163–176
- Matsubara, M., Zieske, J. D., and Fini, M. E. (1991) *Invest. Ophthalmol. Vis. Sci.* **32**, 3221–3237
- Matsubara, M., Girard, M. T., Kublin, C. L., Cintron, C., and Fini, M. E. (1991) *Dev. Biol.* **147**, 425–439
- Legrand, C., Gilles, C., Zahm, J. M., Polette, M., Buisson, A. C., Kaplan, H., Birembaut, P., and Tournier, J. M. (1999) *J. Cell Biol.* **146**, 517–529
- Leppert, D., Waubant, E., Galardy, R., Bunnett, N. W., and Hauser, S. L. (1995) *J. Immunol.* **154**, 4379–4389
- Okada, S., Kita, H., George, T. J., Gleich, G. J., and Leiferman, K. M. (1997) *Am. J. Respir. Cell Mol. Biol.* **17**, 519–528
- Azar, D. T., Pluznik, D., Jain, S., and Khoury, J. M. (1998) *Arch. Ophthalmol.* **116**, 1206–1208
- Gipson, I. K., Spurr-Michaud, S. J., and Tisdale, A. S. (1988) *Dev. Biol.* **126**, 253–262
- Vu, T. H., Shipley, J. M., Bergers, G., Berger, J. E., Helms, J. A., Hanahan, D., Shapiro, S. D., Senior, R. M., and Werb, Z. (1998) *Cell* **93**, 411–422
- Grobely, D., Poncz, L., and Galardy, R. E. (1992) *Biochemistry* **31**, 7152–7154
- Rousselle, P., Lunstrum, G. P., Keene, D. R., and Burgeson, R. E. (1991) *J. Cell Biol.* **114**, 567–576
- Drew, A. F., Schiman, H. L., Kombrinck, K. W., Bugge, T. H., Degen, J. L., and Kaufman, A. H. (2000) *Invest. Ophthalmol. Vis. Sci.* **41**, 67–72
- Gipson, I. K., and Kiorpes, T. C. (1982) *Dev. Biol.* **92**, 259–262
- Giannelli, G., Falk-Marzillier, J., Schiraldi, O., Stetler-Stevenson, W. G., and Quaranta, V. (1997) *Science* **277**, 225–228
- Lund, L. R., Romer, J., Bugge, T. H., Nielsen, B. S., Frandsen, T. L., Degen,

- J. L., Stephens, R. W., and Dano, K. (1999) *EMBO J.* **18**, 4645–4656
45. Fini, M. E., Cui, T. Y., Mouldovan, A., Grobelny, D., Galardy, R. E., and Fisher, S. J. (1991) *Invest. Ophthalmol. Vis. Sci.* **32**, 2997–3001
46. Chin, J. R., and Werb, Z. (1997) *Development* **124**, 1519–1530
47. Betsuyaku, T., Shipley, J. M., Liu, Z., and Senior, R. M. (1999) *Am. J. Respir. Cell Mol. Biol.* **20**, 1303–1309
48. Wang, M., Qin, X., Mudgett, J. S., Ferguson, T. A., Senior, R. M., and Welgus, H. G. (1999) *Proc. Natl. Acad. Sci. U. S. A.* **96**, 6885–6889
49. Chung, E. H., Hutcheon, A. E., Joyce, N. C., and Zieske, J. D. (1999) *Invest. Ophthalmol. Vis. Sci.* **40**, 1952–1958
50. Zagon, I. S., Sassani, J. W., Ruth, T. B., and McLaughlin, P. J. (2000) *Brain Res.* **882**, 169–179
51. Ashcroft, G. S., Yang, X., Glick, A. B., Weinstein, M., Letterio, J. L., Mizel, D. E., Anzano, M., Greenwell-Wild, T., Wahl, S. M., Deng, C., and Roberts, A. B. (1999) *Nat. Cell Biol.* **1**, 260–266
52. Wrana, J. L. (2000) *Cell* **100**, 189–192
53. Strissel, K. J., Rinehart, W. B., and Fini, M. E. (1997) *Invest. Ophthalmol. Vis. Sci.* **38**, 546–552
54. Strissel, K. J., Rinehart, W. B., and Fini, M. E. (1995) *Invest. Ophthalmol. Vis. Sci.* **36**, 151–162
55. Wilson, S. E., Schultz, G. S., Chegini, N., Weng, J., and He, Y. G. (1994) *Exp. Eye Res.* **59**, 63–71
56. Fini, M. (1999) *Prog. Ret. Eye Res.* **18**, 529–551
57. Clark, R. A., Lanigan, J. M., DellaPelle, P., Manseau, E., Dvorak, H. F., and Colvin, R. B. (1982) *J. Invest. Dermatol.* **79**, 264–269
58. Phan, T. M., Foster, C. S., Wasson, P. J., Fujikawa, L. S., Zagachin, L. M., and Colvin, R. B. (1989) *Invest. Ophthalmol. Vis. Sci.* **30**, 377–385
59. Fujikawa, L. S., Foster, C. S., Harrist, T. J., Lanigan, J. M., and Colvin, R. B. (1981) *Lab. Invest.* **45**, 120–129
60. Fujikawa, L. S., Foster, C. S., Gipson, I. K., and Colvin, R. B. (1984) *J. Cell Biol.* **98**, 128–138
61. Nishida, T., Nakagawa, S., Ohashi, Y., Awata, T., and Manabe, R. (1982) *Jpn. J. Ophthalmol.* **26**, 410–415
62. Suda, T., Nishida, T., Ohashi, Y., Nakagawa, S., and Manabe, R. (1981) *Curr. Eye Res.* **1**, 553–556
63. Dinarello, C. A. (1988) *FASEB J.* **2**, 108–115
64. Gipson, I. K., Spurr-Michaud, S., Tisdale, A., and Keough, M. (1989) *Invest. Ophthalmol. Vis. Sci.* **30**, 425–434
65. Betsuyaku, T., Fukuda, Y., Parks, W. C., Shipley, J. M., and Senior, R. M. (2000) *Am. J. Pathol.* **157**, 525–535
66. Roberts, A. B. (1999) *Microbes Infect.* **1**, 1265–1273
67. Hiraoka, N., Allen, E., Apel, I. J., Gyetko, M. R., and Weiss, S. J. (1998) *Cell* **95**, 365–377
68. Jester, J. V., Moller-Pedersen, T., Huang, J., Sax, C. M., Kays, W. T., Cavangh, H. D., Petroll, W. M., and Piatigorsky, J. (1999) *J. Cell Sci.* **112**, 613–622
69. Gartry, D. S., Kerr Muir, M. G., and Marshall, J. (1992) *Ophthalmology* **99**, 1209–1219
70. Maguen, E., Salz, J. J., Nesburn, A. B., Warren, C., Macy, J. I., Papaioannou, T., Hofbauer, J., and Berlin, M. S. (1994) *Ophthalmology* **101**, 1548–1557
71. Schallhorn, S. C., Blanton, C. L., Kaupp, S. E., Sutphin, J., Gordon, M., Goforth, H., Jr., and Butler, F. K., Jr. (1996) *Ophthalmology* **103**, 5–22
72. Seiler, T., Holschbach, A., Derse, M., Jean, B., and Genth, U. (1994) *Ophthalmology* **101**, 153–160
73. Sher, N. A., Hardten, D. R., Fundingsland, B., DeMarchi, J., Carpel, E., Doughman, D. J., Lane, S. S., Ostrov, C., Eiferman, R., and Frantz, J. M. (1994) *Ophthalmology* **101**, 1575–1582
74. Falanga, V., Grinnell, F., Gilchrist, B., Maddox, Y. T., and Moshell, A. (1994) *J. Invest. Dermatol.* **102**, 125–127
75. Falanga, V., and Eaglstein, W. H. (1993) *Lancet* **341**, 1006–1008
76. Bitzer, M., Gersdorff, G. B., Liang, D., Dominguez-Rosales, A., Beg, A. A., Rojkind, M., and Bottinger, E. P. (2000) *Genes Dev.* **14**, 187–197
77. Brown, J. D., DiChiara, M. R., Anderson, K. R., Gimbrone, M. A., Jr., and Topper, J. N. (1999) *J. Biol. Chem.* **274**, 8797–8805
78. Pick, E., Ju, W. J., Heyer, J., Escalante-Alcalde, D., Stewart, C. L., Weinstein, M., Deng, C., Kucherlapati, R., Bottinger, E. P., and Roberts, A. B. (2001) *J. Biol. Chem.* **276**, 19945–19953
79. Liu, Z., Zhou, X., Shapiro, S. D., Shipley, J. M., Twining, S. S., Diaz, L. A., Senior, R. M., and Werb, Z. *Cell* **102**, 647–655
80. Labbe, E., Silvestri, C., Hoodless, P. A., Wrana, J. L., and Attisano, L. (1998) *Mol. Cell* **2**, 109–120
81. Sun, Y., Liu, X., Eaton, E. N., Lane, W. S., Lodish, H. F., and Weinberg, R. A. (1999) *Mol. Cell* **4**, 499–509